

## ULTRA-WIDEBAND TRACKING OF MOBILE ROBOTS WITH VIDEO VALIDATION

**Ka C Cheok, PhD**  
**Micho T Radovnikovich**  
**Pavan K Vempaty**  
ECE Dept  
Oakland University  
Rochester, MI

**Gregory R Hudas, PhD**  
**James L Overholt, PhD**  
Joint Center for Robotics  
US Army TARDEC  
Warren, MI

**Paul W Fleck**  
Dataspeed Inc  
Troy, MI

### ABSTRACT

*Ultra-wideband (UWB) radio ranging technology was integrated into a local positioning system (LPS) for tracking mobile robots. A practical issue was the occasional large sporadic errors in the radio range data due to multipath due to reflections and attenuation effect caused by radio penetration through mediums. In this paper, we present a filtering and system integration of the radios with vehicle sensors to produce location and orientation of a moving object being tracked. We introduced a fuzzy neighborhood filter to remove outliers from range data, a progressive trilateration filter to improve update rate and produce a fused estimate of vehicle location with a compass and wheel speed sensors. Experiments were recorded and estimated position and orientation were validated against the video recording of vehicle ground truth. The UWB LPS can be used for navigation and guidance of multiple mobile robots around a command vehicle, and employed for tracking of assets of interest including personnel, vehicle, weapons and equipment.*

### 1 INTRODUCTION

Recent ultra-wideband (UWB) radio ranging technology [1]–[3] can be integrated into an ad-hoc local positioning system (LPS) [4]–[6] for the purpose of tracking personnel, vehicles and assets in a new environment. The LPS works in indoors and outdoors environments, and can range through objects (such as walls, foliage, bodies, etc.) to a certain extent. It can be a standalone system or complementary system to the Global Positioning System (GPS), especially where GPS is unavailable or denied. This paper presents an LPS that employs ultra-wideband (UWB) ranging radios for tracking mobile robots<sup>1</sup>.

A major practical issue with the new technology is the occasional large sporadic errors in the radio range data

due to multipath due to reflections and attenuation effect caused by radio penetration through mediums. This paper describes a theoretical basis for a UWB LPS addressing the issues. The LPS was implemented and verified through experiments. Validation of the LPS estimates was verified using video record of ground truth.

### 2 PROBLEM STATEMENT

The LPS employs P210 UWB radios from Time Domain Inc. See Fig. 1. The technology uses a time-of-arrival method for measuring time-of-flight of UWB pulse between the radios, and has a range up to 100 meters under FCC regulation +10 db power, with a quantized resolution of 15 cm. The radios operate with a center frequency of



Fig. 1: P210 UWB ranging radio

<sup>1</sup> This research is sponsored by the Joint Center for Robotics of the US Army TARDEC

4.7 GHz and bandwidth of 3.2 GHz. They communicated via Ethernet connection using the user datagram protocol (UDP) controlled to a PC.

The base station radios are set up on a custom-built cart to allow quick and easy assembly and disassembly of the base station. The position of the arms holding the radios can be adjusted to allow the testing of various configurations. The cart also contains a stand to hold the laptop which communicates with the radios. Each of the four arms of the base station holds a P210 UWB radio that is positioned parallel to the ground. These radios from the base station trilaterate in real time with the fifth UWB radio that is attached to a Mecanum omnidirectional vehicle (ODV), and the location is derived for tracking. The experimental setup with the base station and the mobile robot are shown in Fig 2.



Fig. 2: UWB base station test rig and Mecanum ODV

In this paper, we developed an LPS algorithm that incorporates i) a fuzzy neighborhood filter for removing the outliers from range data [7, 13], ii) a progressive trilateration filter for improving the update rate, and iii) a sensor fusion estimator for the vehicle position and orientation that combines the UWB radios with a compass and wheel speed sensors. Experiments were carried out where the LPS was applied to navigate and guidance of an omnidirectional vehicle. Recorded video data were used to validate the fused trilateration results.

The practical realization in this paper includes: application of the new UWB ranging radio technology; Matlab/Simulink implementation the LPS algorithm; automatic base station calibration; experimental mobile

robot test rigs to verify the results; and validation of theoretical simulation and practical experimental results against video evidence of the ground truth of the mobile robot.

### 3 OUTLIER FILTERING

Radio range data can be seriously corrupted, resulting in erroneous sporadic larger ranges caused by multipath reflections of radio waves off the walls, ceiling, floor and objects, as well as attenuation effect caused by radio penetrating through mediums [3]. Fig. 3 shows a block diagram of the fuzzy neighborhood tracking scheme [7] has successfully proven to clean up the UWB measurements. A fuzzy logic tuned double Kalman filter (KF) tracker configuration [8]-[10] is based on the phenomenon that the physical distance between UWB radios changes according to an  $\alpha - \beta$  motion model described by

$$\mathbf{x}_{r,k+1} = \mathbf{A}_r \mathbf{x}_{r,k} + \mathbf{G}_r w_k \quad (1)$$

$$\mathbf{y}_{r,k+1} = \mathbf{C}_r \mathbf{x}_{r,k} + v_k$$

$$\mathbf{x}_{r,k} = \begin{bmatrix} x_{r,k} \\ \dot{x}_{r,k} \end{bmatrix}, \mathbf{C}_r = \begin{bmatrix} 1 & 0 \end{bmatrix}, \mathbf{A}_r = \begin{bmatrix} 1 & T_s \\ 0 & 1 \end{bmatrix}, \mathbf{G}_r = \begin{bmatrix} 0 \\ T_s \end{bmatrix}$$

where  $x_{r,k}$  and  $\dot{x}_{r,k}$  represents displacement and speed,  $T_s$  the sampling interval,  $w_k$  changes in speed and  $v_k$  the measurement noise. We suppose that the speed changes infrequently so that  $w_k$  is a sparse sporadic noise. Let the mean and covariance of  $w_k$  and  $v_k$  be denoted  $\bar{w}$  and  $\bar{v}$ , and  $Q_w$  and  $R_v$ , respectively. For the motion of the target unit being considered, we assume that  $\bar{w}$  and  $\bar{v}$  and  $Q_w$  and  $Q_v$  are known or have been characterized. We also assume that the noises are generally Gaussian. The **OKF**, whose update equations are given by (2), is tuned with  $Q_{w0} = 10^2 Q_w$  to reflect anticipated fast movement of mobile radio and  $R_{v0} = R_v$  to reflect normal spread of the measured ranges. The **NKF**, whose update equations are given by (3), is tuned with  $Q_{wN} = Q_w$  to reflect the expected regular movement of the object and  $R_{vN} \leq R_v$  to reflect the higher trust in the new selective neighborhood measurement.

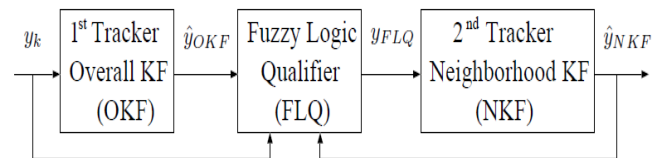


Fig. 3: Fuzzy neighborhood tracking filters

The FLQ fuzzy rules [11]-[12] are defined as

**Rules :**

$$\begin{aligned}
 &\text{If } |y_{r,k} - \hat{y}_{OKF,k}| \text{ is small, then } y_{FLQ,k} = y_{r,k} \\
 &\text{If } |y_{r,k} - \hat{y}_{OKF,k}| \text{ is large, then } y_{FLQ,k} = y_{NKF,k} \\
 &\mathbf{x}_{O,k/k} = \mathbf{x}_{O,k/k-1} + \mathbf{K}_{O,k} (y_{r,k} - \mathbf{C}_r \mathbf{x}_{O,k/k-1}) \\
 &\mathbf{x}_{O,k+1/k} = \mathbf{A}_r \mathbf{x}_{O,k/k} \\
 &\hat{y}_{OKF,k} = \mathbf{C}_r \mathbf{x}_{N,k/k} \\
 &\mathbf{x}_{N,k/k} = \mathbf{x}_{N,k/k-1} + \mathbf{K}_{N,k} (y_{FLQ,k} - \mathbf{C}_r \mathbf{x}_{N,k/k-1}) \\
 &\mathbf{x}_{N,k+1/k} = \mathbf{A}_r \mathbf{x}_{N,k/k} \\
 &\hat{y}_{NKF,k} = \mathbf{C}_r \mathbf{x}_{N,k/k}
 \end{aligned} \tag{2}$$

#### 4 TRILATERATION

Using four UWB ranging radios, it is possible to trilaterate the position of a fifth radio uniquely. In this paper, the fifth radio is defined as the ‘target’ radio, and the four others are the ‘base station.’ The distance between the target radio and each base station radio is measured, and used to compute the position of the target. The position of the target radio is measure according to

$$\begin{aligned}
 &\mathbf{Z}_k = \mathbf{C}_x \mathbf{x} \\
 &\mathbf{C}_x = 2 \begin{bmatrix} x_{21} & y_{21} & z_{21} \\ x_{32} & y_{32} & z_{32} \\ x_{43} & y_{43} & z_{43} \\ x_{14} & y_{14} & z_{14} \end{bmatrix} \\
 &\mathbf{Z}_k = \begin{bmatrix} (x_2^2 - x_1^2) + (y_2^2 - y_1^2) + (z_2^2 - z_1^2) - (r_2^2 - r_1^2) \\ (x_3^2 - x_2^2) + (y_3^2 - y_2^2) + (z_3^2 - z_2^2) - (r_3^2 - r_2^2) \\ (x_4^2 - x_3^2) + (y_4^2 - y_3^2) + (z_4^2 - z_3^2) - (r_4^2 - r_3^2) \\ (x_1^2 - x_4^2) + (y_1^2 - y_4^2) + (z_1^2 - z_4^2) - (r_1^2 - r_4^2) \end{bmatrix}
 \end{aligned} \tag{4}$$

where  $\mathbf{x} = [x \ y \ z]^T$  is the computed location of the target radio,  $r_1$  through  $r_4$  are the range measurements from each base station radio, and the numbered  $x, y$  and  $z$  are the previously known coordinates of each base station radio.  $x_{i,j}, y_{i,j}$  and  $z_{i,j}$  are shorthand for  $x_i - x_j, y_i - y_j$  and  $z_i - z_j$ , respectively. (4) is derived from the time of arrival (TOA) principle [5].

#### 4.1 Automatic Base Station Calibration

To trilaterate the position of the target radio, (4) requires the coordinates of the four base station radios. In order to easily and accurately set up the base station and obtain these coordinates, a system is presented to automatically detect the configuration of the radios. This system is based on an algorithm that derives the coordinates of the base station radios using only measurements of the distances between each radio [4]. The coordinates of first base station radio are defined at the origin, the line between the first and second radios is defined as the  $x$  axis ( $y = 0$ ), and the plane containing the first three radios is defined as the  $x - y$  plane ( $z = 0$ ). Based on these assumptions:

$$\begin{aligned}
 &x_1 = 0, y_1 = 0, z_1 = 0 \\
 &x_2 = l_{12}, y_2 = 0, z_2 = 0 \\
 &x_3 = \frac{l_{12}^2 + l_{13}^2 - l_{23}^2}{2l_{12}}, y_3 = \sqrt{l_{13}^2 - x_3^2}, z_3 = 0 \\
 &x_4 = \frac{l_{12}^2 + l_{14}^2 - l_{24}^2}{2l_{12}} \\
 &y_4 = \frac{(x_3 - x_4)^2 + y_3^2 + l_{14}^2 - x_4^2 - l_{34}^2}{2y_3} \\
 &z_4 = \sqrt{l_{34}^2 - (x_3 - x_4)^2 - (y_3 - y_4)^2}
 \end{aligned} \tag{5}$$

where  $l_{ij}$  is the measured distance between radios  $i$  and  $j$ , and  $x_n, y_n$  and  $z_n$  are the coordinates of base station radio  $n$ . However, since the coordinates in (5) are based on the  $x - y$  plane defined by the first three radios, they must be transformed into the ground frame. This is done by finding the rotation matrix between the radio and ground frames by inputting manual measurements of the heights of the first three radios. Euler angle rotation matrices for  $x$  and  $y$  are computed individually and are then multiplied:

$$\mathbf{R} = \mathbf{R}_y \mathbf{R}_x = \begin{bmatrix} c\theta & 0 & s\theta \\ 0 & 1 & 0 \\ -s\theta & 0 & c\theta \end{bmatrix} \begin{bmatrix} 1 & 0 & 0 \\ 0 & c\rho & s\rho \\ 0 & -s\rho & c\rho \end{bmatrix} \tag{6}$$

where the roll angle  $\rho$  and pitch angle  $\theta$  are given by

$$\rho = \sin^{-1} \left( \frac{h_2 - h_3}{l_{23}} \right), \theta = \sin^{-1} \left( \frac{h_2 - h_1}{l_{12}} \right) \tag{7}$$

#### 4.2 Progressive Update Trilateration Filter

With (4), all four base station radios need to make measurements with the target radio before the position estimate of the target can be updated. This causes very slow updating of the position estimate, which experiments have shown to be very prohibiting to achieve good tracking of a moving target. Therefore, a progressively updating filter was developed to make predictions of the target's position after each measurement is made. This provides a four times faster update rate over the direct use of (4). A state space model for the system is developed that treats the  $x, y$  and  $z$  position and velocity of the target radio as states, using standard first order dynamics. The state equations can be formed by rearranging (4). Doing this, the state space model is given by (8), where  $\mathbf{Z}_k$  is the current value of the second matrix in (4), containing the distance measurements from the base station radios.

$$\begin{aligned} \begin{bmatrix} \mathbf{x}_k \\ \dot{\mathbf{x}}_k \end{bmatrix}_{k+1} &= \mathbf{A} \begin{bmatrix} \mathbf{x}_k \\ \dot{\mathbf{x}}_k \end{bmatrix}_k \\ \mathbf{Z}_k &= \mathbf{C} \begin{bmatrix} \mathbf{x}_k \\ \dot{\mathbf{x}}_k \end{bmatrix}_k \\ \mathbf{A} &= \begin{bmatrix} \mathbf{I}_3 & T_s \mathbf{I}_3 \\ \mathbf{0}_{3 \times 3} & \mathbf{I}_3 \end{bmatrix}, \mathbf{C} = [\mathbf{C}_x \quad \mathbf{0}_{4 \times 3}] \end{aligned} \quad (8)$$

The filter update equation is then

$$\mathbf{X}_{k+1} = \mathbf{A}\mathbf{X}_k + \mathbf{L}(\mathbf{Z}_k - \mathbf{C}\mathbf{X}_k) \quad (9)$$

where  $\mathbf{X} = [\mathbf{x} \quad \dot{\mathbf{x}}]$ , and the gain matrix  $\mathbf{L}$  is designed such that the observer characteristic matrix  $\mathbf{A} - \mathbf{L}\mathbf{C}$  contains certain stable poles. These poles are adjusted to yield the best convergence properties of the trilateration filter. In order to make an estimate after every range reading, (9) is used with the column of the  $\mathbf{L}$  matrix and the row of the  $\mathbf{C}$  matrix that correspond to the measurement that is being made. Therefore, (9) is modified to

$$\mathbf{X}_{k+1} = \mathbf{A}\mathbf{X}_k + \mathbf{L}_n (\mathbf{Z}_{kn} - \mathbf{C}_n \mathbf{X}_k), \quad n = 1, 2, 3, 4 \quad (10)$$

where  $\mathbf{L}_n$  is the  $n^{\text{th}}$  column of  $\mathbf{L}$  and  $\mathbf{Z}_{kn}$  is the measurement value from the  $n^{\text{th}}$  radio, and  $\mathbf{C}_n$  is the  $n^{\text{th}}$  row of  $\mathbf{C}$ .

## 5 KALMAN FILTER BASED SENSOR FUSION

To track a mobile robot sufficiently, trilateration on its own is not enough information. The position estimate from

trilateration tends to be quite noisy, especially when the Target is moving. Because of this, it is almost impossible to track the heading of the mobile robot with the raw position estimate.

To correct this problem, an Extended Kalman Filter (EKF) is developed to fuse the trilateration measurements with headings from other sensors on the mobile robot platform, namely wheel speed encoders and a digital compass. This section discusses the modeling of the system, and the derivation of the Kalman Filter.

### 5.1 Mecanum Drive Mobile Robot

The mobile robot platform used to test the system is an omnidirectional vehicle using Mecanum wheels. The Mecanum drive system consists of four fixed, independently controlled wheels. The contact surface of each wheel is a series of rollers, each oriented at 45 degrees to the wheel's axis of rotation. When the wheel is rotated, the rollers spin freely while applying force along their axis of rotation. By controlling the speed and direction of the four wheels separately, these diagonal forces can be combined to allow the vehicle to move in any direction while at the same time controlling its rotational speed. Fig. 4 shows an illustration of a Mecanum ODV defining the nomenclature of the variables of motion and the geometry of the kinematics model. The rotational speeds of the wheels are given by  $\omega_1$  through  $\omega_4$ , and the positive direction of rotation corresponds to the dashed arrows in Fig. 4. The solid arrows represent the force applied by the given wheel, and  $v_x, v_y$  and  $\omega_z$  are the velocities in each of the three degrees of freedom of the ODV.

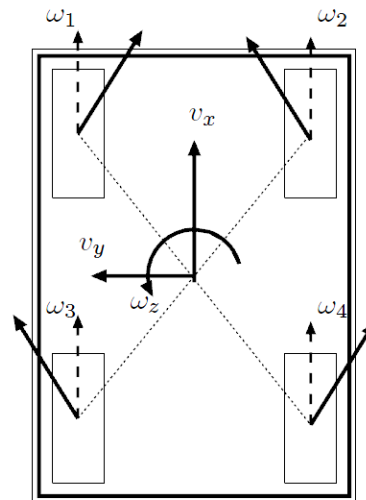


Fig. 4: Illustration of the Mecanum ODV Platform

The kinematic relationship between the wheel rotation speeds and the vehicle's motion can be defined using a single matrix transformation:

$$\begin{bmatrix} \omega_1 \\ \omega_2 \\ \omega_3 \\ \omega_4 \end{bmatrix} = \begin{bmatrix} a_1 & b_1 & c_1 \\ a_2 & b_2 & c_2 \\ a_3 & b_3 & c_3 \\ a_4 & b_4 & c_4 \end{bmatrix} \begin{bmatrix} v_x \\ v_y \\ \omega_z \end{bmatrix} \quad (11)$$

The parameters of the matrix in Equation (11) are the ratios between the amounts of wheel rotation per amount of travel in a given axis. For example, the parameter  $b_2$  is the amount wheel two rotates when the vehicle moves a unit distance in the  $y$  direction.

## 5.2 System Model

Fig. 5 shows a diagram from which the model equations are derived. The  $x$  and  $y$  axes represent the reference frame defined by the UWB base station configuration. The heading of the robot is represented by  $\theta$ , the omnidirectional direction of travel is given by  $\phi = \tan^{-1}\left(\frac{v_y}{v_x}\right)$ , and the direction of travel in the UWB frame is given by  $\psi = \theta + \phi$ . The velocity of the vehicle is given by  $v_x, v_y$  and  $\omega_z$ , and are the same as in Equation (11). The vehicle's velocity in the UWB reference frame are given by  $\dot{x}, \dot{y}$  and  $\dot{\theta}$ . From Fig. 5, it can be seen that

$$\begin{aligned} \dot{x} &= v_x \cos \theta - v_y \sin \theta, & \dot{x} &= v \cos \psi \\ \dot{y} &= v_x \sin \theta + v_y \cos \theta, & \dot{y} &= v \sin \psi \end{aligned} \quad (12)$$

Where  $v = \sqrt{v_x^2 + v_y^2}$ . (12) provides a basis for the Kalman Filter. The system state vector is  $\mathbf{X}_F = [x \ \dot{x} \ y \ \dot{y} \ \theta \ \dot{\theta} \ b]^T$ , where  $b$  represents the offset between the compass heading measurement and the heading of the vehicle in the UWB frame. The input vector to the system is  $\mathbf{U} = [v_x \ v_y]^T$ , which is the velocity of the vehicle as measured by the wheel encoders. Using these definitions, the state equations are defined in (13). Then, using the measurements from all the sensors and

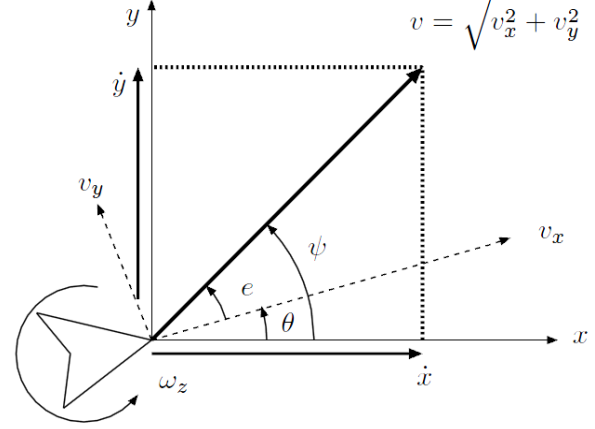


Fig. 5: Diagram outlining the kinematics of the mobile robot in UWB reference frame

making use of more information from the kinematics, the measurement equations and state observation matrix can be constructed as shown in (15) and (16). This non-linear system is then linearized using a Taylor Series approximation, as shown in (14).

$$\dot{\mathbf{X}}_F = f(\mathbf{X}_F, \mathbf{U}) = \begin{cases} v_x \cos \theta - v_y \sin \theta \\ 0 \\ v_x \sin \theta + v_y \cos \theta \\ 0 \\ \dot{\theta} \\ 0 \\ 0 \end{cases} \quad (13)$$

$$\Delta \dot{\mathbf{X}}_F = \left. \frac{\partial f}{\partial \mathbf{X}_F} \right|_{\substack{\mathbf{X}_F = \mathbf{X}_{F,0} \\ \mathbf{U} = \mathbf{U}_0}} \Delta \mathbf{X}_F + \left. \frac{\partial f}{\partial \mathbf{U}} \right|_{\substack{\mathbf{X}_F = \mathbf{X}_{F,0} \\ \mathbf{U} = \mathbf{U}_0}} \Delta \mathbf{U} \quad (14)$$

The measurements used in the Kalman Filter include the  $x$  and  $y$  position estimate from the trilateration filter, the rotation speed of the vehicle as measured from the wheel encoders, and the heading of the vehicle as measured by the digital compass. As such, the measurement equation and observation matrix of the EKF are given by (15) and (16), respectively.

$$\mathbf{Z}_{F,K} = h(\mathbf{X}_F, \mathbf{U}) = \begin{cases} x \\ y \\ \dot{\theta} \\ \theta + b \end{cases} \quad (15)$$

$$H_k = \frac{\partial h}{\partial \mathbf{X}} = \begin{bmatrix} 1 & 0 & 0 & 0 & 0 & 0 & 0 \\ 0 & 0 & 1 & 0 & 0 & 0 & 0 \\ 0 & 0 & 0 & 0 & 0 & 1 & 0 \\ 0 & 0 & 0 & 0 & 1 & 0 & 1 \end{bmatrix} \quad (16)$$

The recursive Extended Kalman Filter algorithm then follows the following procedure, where  $Q$  is the modelled random process noise covariance matrix and  $R$  is the measurement noise covariance matrix:

1) Predict state:

$$\mathbf{X}_{F,k|k-1} = f(\mathbf{X}_{F,k-1|k-1}, \mathbf{U}_k)$$

2) Predict estimate covariance:

$$P_{k|k-1} = F_k P_{k-1|k-1} F_k^T + Q$$

3) Update residual covariance:

$$S_k = H_k P_{k|k-1} H_k^T + R$$

4) Compute Kalman gain:

$$K_k = P_{k|k-1} H_k^T S_k^{-1}$$

5) Update state estimate:

$$\mathbf{X}_{F,k|k} = \mathbf{X}_{F,k|k-1} + K_k (Z_{F,k} - h(\mathbf{X}_{F,k|k-1}))$$

## 6 EXPERIMENTS

### 6.1 A. Experimental Setup

The UWB tracking system described in the previous sections was implemented using the base station cart and Mecanum ODV as described in Section II. A diagram of the hardware architecture used in the experiments is shown in Fig. 6. The software diagram is shown in Fig. 7.

### 6.2 Outlier Removal Results

The FNTF was applied to experimental data in the test pavilion. Fig. 8 shows the raw ranges collected cover 20 to 200 ft at intervals of 20 ft. It is seen that the large sporadic multipath noise are more prominent over the ranges between 20 to 100 ft and they ease off at ranges above that. Fig. 9 shows the clean output of the neighborhood tracking filter (NKF) that uses the qualified selected measurements. It is seen that the FNTF has completely removed the erroneous noise.

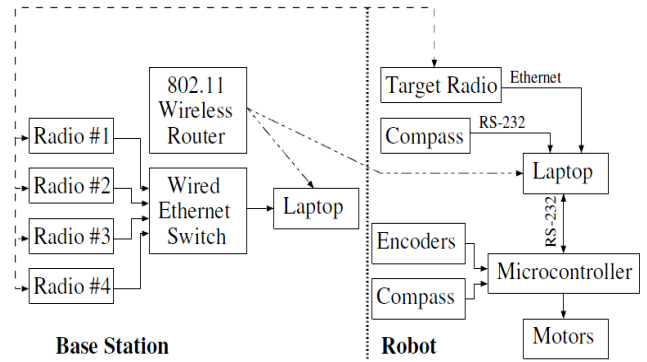


Fig. 6: Hardware architecture used in UWB tracking experiments

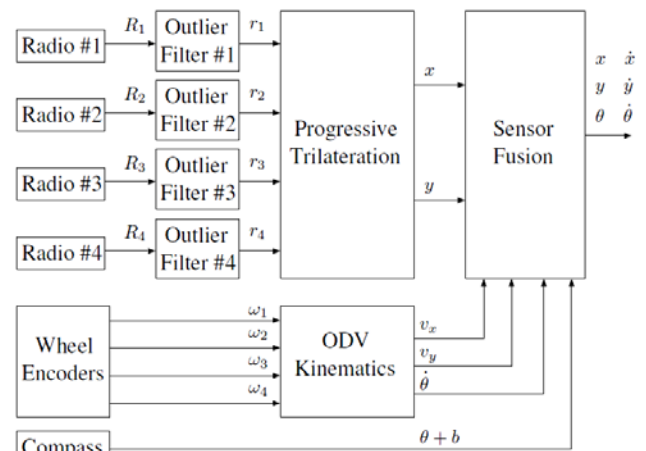


Fig. 7: Software diagram for UWB tracking with sensor fusion

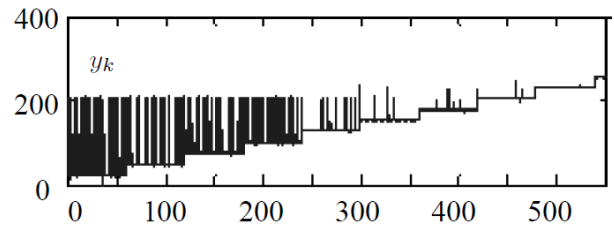


Fig. 8: Raw ranges with large sporadic multipath errors

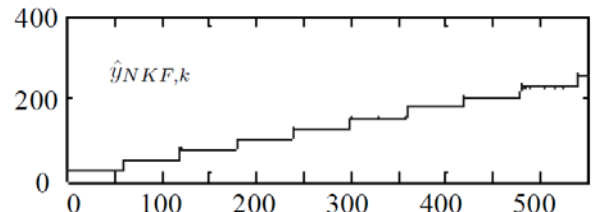


Fig. 9: Experimental data and effectiveness of Fuzzy Neighborhood Tracking Filters

### 6.3 Video-Based Ground Truth Verification

In order to verify the results from the trilateration experiments, videos of the live experiments were synchronized with the data gathered during the experiment. The video frames were transformed to make it appear that the video was taken directly from overhead, so that the ground truth data from the images is simpler to extract and easier to visualize. This transformation is illustrated geometrically in Fig. 10. The transformation stages were calibrated using some simple distance measurements. Each pixel in the original image is processed through the transformation and remapped into the top-view image. A sample of the transformation procedure is shown in Fig. 11.

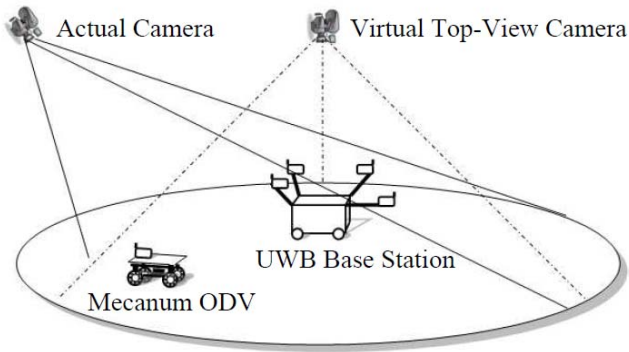


Fig. 10: Diagram illustrating the image transformation procedure

### 6.4 Trilateration Results

The UWB tracking system presented in this paper was implemented using the hardware architecture from Fig. 6 and the three-layer filtering technique illustrated in Fig. 7. The estimates from the filtering scheme are overlaid on the synchronized video frames to verify their accuracy. Fig. 12 shows these plots, where the  $x$  and  $y$  estimates are a dark grey trail showing where the ODV has been previously, and the  $\theta$  heading angle estimate is represented by the thick black line.

## 7 CONCLUSION

The UWB ranging radios were capable of precise and accurate measurement in static and uncluttered environment. However, the range measurements become inherently sporadic and a drawback when subjected to multipath and attenuation especially if the radios are moving. This paper showed how UWB ranging radios and vehicle sensors were combined to produce a local positioning system for tracking of a moving mobile robot. The estimate of the robot location and orientation were generated by a three-layer filtering scheme: the fuzzy neighborhood filter, the progressive

trilateration filter and the sensor fusion filter. In this paper, we verified the validity of the UWB-based LPS estimate against the actual path of the robot via juxtaposing the results against video evidence.

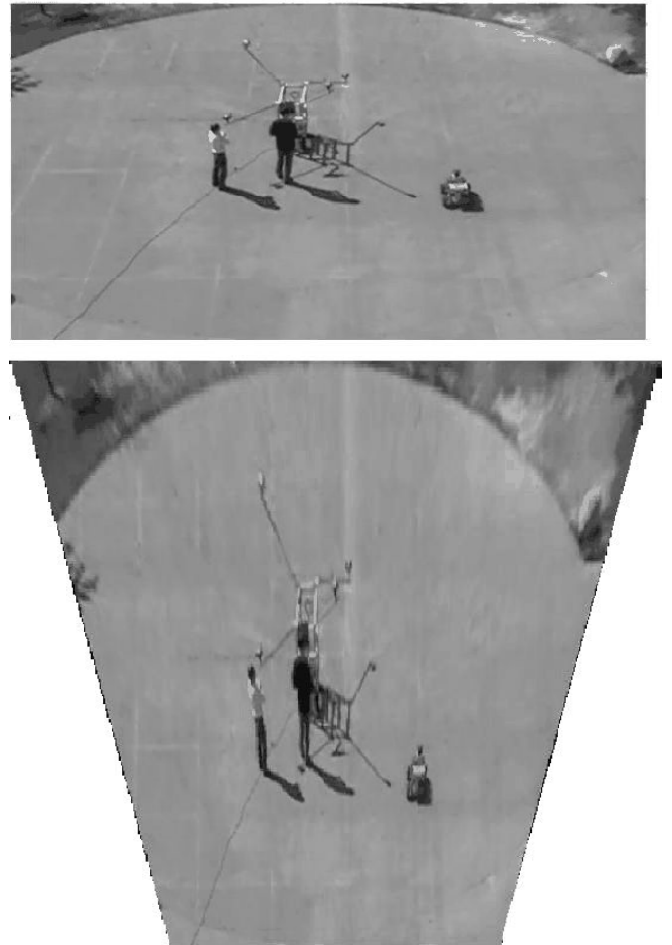
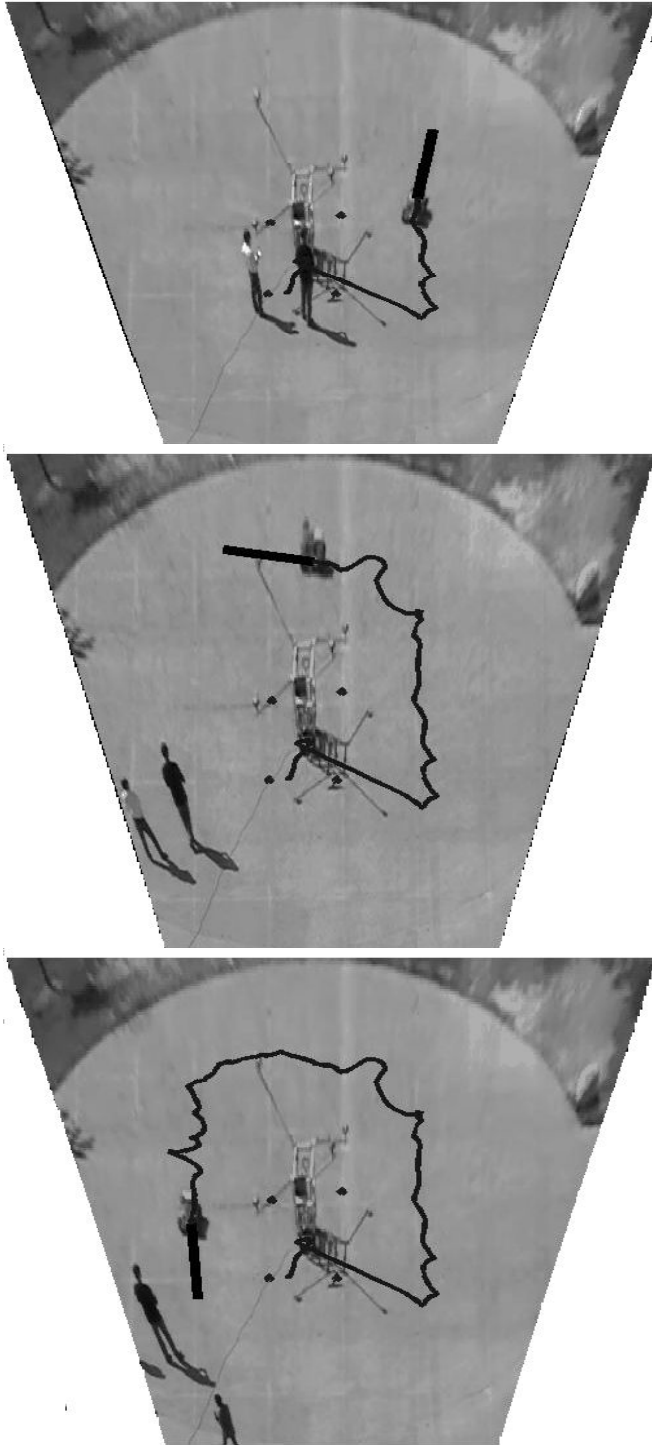


Fig. 11: Input image and output top-view image



## REFERENCES

- [1] R. J. Fontana, "Recent systems applications of short-pulse ultrawideband technology," *IEEE Microwave Theory & Technology*, vol. 52, no. 9, September 2004.
- [2] R. J. Fontana, E. Richley, and J. Barney, "Commercialization of an ultra wideband precision asset location system," in *Proc. of the 2003 IEEE Conference on Ultra Wideband Systems and Technologies*, Reston, VA, 2003.
- [3] V. S. Sonwalkar, A. Venkatasubramanian, B. A. Johnson, and J. G. Hawkins, "UWB propagation over the ground," Electrical & Computer Eng. Dept., University of Alaska Fairbanks, Fairbanks AK-99775, USA.
- [4] K. C. Cheok, "Navigation system," US Patent No: US 7,403,783 B2, February 2004.
- [5] K. C. Cheok, B. Liu, G. R. Hudas, J. L. Overholt, and M. Skalny, "Ultrawideband methods for UGV positioning: Experimental and Simulation Results," *Procs. of 2006 US Army Science Conference*, 2006.
- [6] G. R. Hudas, J. Overholt, K. C. Cheok, and G. Smid, "TOA & TDOA method for UWB RF location technique," *Procs. of 2004 US Army Science Conference*, Orlando, FL, 2004.
- [7] K. C. Cheok, "Ultra-wideband (UWB) local positioning system (LPS) an experimental study and analysis," in *Procs of 2008 WAC ISSCI (Soft Computing)*, Waikoloa, HA, September 2008.
- [8] A. Gelb, Ed., *Applied Optimal Estimation*, 16th ed. Cambridge, Massachusetts: MIT Press, 2001, pp. 182–192.
- [9] G. R. Hudas, "Statistical test point estimation techniques for nonlinear systems," Ph.D. dissertation, Oakland University, Dept. of Electrical and Systems Engineering, 2003.
- [10] G. R. Hudas, K. C. Cheok, and J. L. Overholt, *NAFIPS'05 Special Issue of the Int. J. of Approximate Reasoning*. Elsevier, 2006, ch. Fuzzy Variant of a Statistical Test Point Kalman Filter.
- [11] J. L. Overholt, K. C. Cheok, and G. E. Smid, "Threshold fuzzy systems: A priority based hierarchical control scheme," *Proc. of the 1999 American Control Conference (ACC)*, San Diego, USA, 1999.
- [12] —, "Control of multi-objective plants using threshold fuzzy systems: Basic concepts," in *World Automation Congress (WAC)*, Alaska, 1998.
- [13] K. C. Cheok, G. R. Hudas, and J. L. Overholt, "Fuzzy neighborhood tracking filters for uwb range radios in multipath environments," in *Proc. of the 2008 SPIE Defense & Security Conference*, Orlando, FL, March 2008.

Fig. 12: UWB Tracking results overlaid over top-view video data